

# Layer-Oriented Wavefront Sensor for MAD: Status and Progress

Elise Vernet Viard<sup>\*,a</sup>, Roberto Ragazzoni<sup>a,b</sup>, Carmelo Arcidiacono<sup>c</sup>, Andrea Baruffolo<sup>d</sup>,  
Emiliano Diolaiti<sup>e</sup>, Jacopo Farinato<sup>a</sup>, Enrico Fedrigo<sup>f</sup>, Enrico Marchetti<sup>f</sup>,  
Renato Falomo<sup>d</sup>, Simone Esposito<sup>a</sup>, Marcel Carbillet<sup>a</sup>, Christophe Vérinaud<sup>a</sup>

<sup>a</sup> INAF- Osservatorio Astrofisico di Arcetri, Italy;

<sup>b</sup>Max Planck Institut für Astronomie – Heidelberg, Germany;

<sup>c</sup>Dipartimento di Astronomia e Fisica dello Spazio, Università di Firenze, Italy;

<sup>d</sup>INAF- Osservatorio Astronomico di Padova, Italy;

<sup>e</sup>Dipartimento di Astronomia, Università di Padova, Italy;

<sup>f</sup>European Southern Observatory, Germany

## ABSTRACT

A demonstrator of the multi-conjugate adaptive optics concept is under construction at ESO and will be installed on the Nasmyth focus of the VLT. This demonstrator called MAD will have two different wavefront sensor channels: Shack-Hartmann and Layer-Oriented; in this article we only describe the Layer-Oriented one. The Layer-Oriented wavefront sensor can select eight reference stars in the two arc-minutes corrected field of view in order to have a maximum of two references in each quarter of the field. XY stages will remotely adjust the position of each reference star selector. The starlight will be fed onto two detectors and two completely independent loops will drive the deformable mirrors, one conjugated to the ground and the other to an altitude of approximately 8 km. The Layer-Oriented wavefront sensor will use the same CCDs than the Shack-Hartmann channel and the pupil will be divided into 9×9 subapertures both for the high and for the ground layer. The spatial sampling of the subapertures will be different for the two CCDs and their integration time will be tuned to typical values of the conjugated altitudes characteristic wind speed. The overall status of the instrument with respect to optics, mechanics, electronics and software is given hereafter. We also summarize the progress on the procurement phase and give the time schedule for the assembling, integration and testing phases.

Keywords: Layer Oriented, Multi Conjugate Adaptive Optics, WaveFront Sensor.

## 1. INTRODUCTION

The Multi-Conjugate Adaptive optics (MCAO) concept was first proposed by Beckers<sup>1,2</sup> in 1987 and 1988. He showed that using several guide stars and several correctors one can map the 3D atmosphere and compensate for the phase distortion in a “3D” fashion. The resulting correction is more uniform over the Field-of-View (FoV). This has been extensively simulated by several groups<sup>3, 4, 5, 6</sup> in the last years and several MCAO instruments<sup>7, 8, 9, 10</sup> are currently in their design phase.

Ragazzoni<sup>11, 12</sup> introduced in 1999 and 2000 a new WF sensing method in MCAO called Layer-Oriented (LO). In the LO way each WFS is conjugated to a specific atmospheric layer instead of being coupled to a reference star like in a classical MCAO. The guide stars light is optically combined by the instrument to reproduce an anamorphic copy of the 3D atmosphere in the pupil plane: the number of DM is equal to the number of WFSs. Each WFS gives then the optimum information to drive independently the DM conjugated to the same layer: the spatial and the temporal samplings of each loop can be optimized according to the statistical properties of the layer.

---

\* For more information, contact the author Elise Vernet. Email: [elise@arcetri.astro.it](mailto:elise@arcetri.astro.it), Phone: +39 055 27 52 273, fax: +39 055 22 00 39. INAF – Osservatorio Astrofisico di Arcetri, I-50125 Firenze

Even though different kind of WFS could be used, the Pyramid Wavefront Sensor<sup>13</sup> (PWFS) has always been associated to the LO concept because it is a pupil plane WFS (well suitable for LO) and because of its gain in sensitivity<sup>18</sup> with respect to others WFSs. The PWFS<sup>14, 15, 16, 17</sup> is a 2D Foucault-like WFS which measures directly the atmospheric distortion in the pupil plane. The first PWFS is working at the Telescopio Nazionale Galileo<sup>16</sup> (TNG) since 2000 and in the last six months is routinely achieving good results: many long exposure images diffraction limited with Strehl values ranging from 15% to 40% (star magnitudes between 10 and 5 in V band) have been secured and the data analysis is in progress in this period. The promising results and unique features (i.e. sensitivity in gain) of the PWFS have generated an increasing interest on this sensor which will be used in one of the two WFS channels of the ESO MCAO demonstrator. Indeed, due to the increasing interest around MCAO (important though not essential for the 8-10m class telescopes, it is unavoidable for the Extremely Large Telescopes - ELTs), the European Southern Observatory (ESO) decided to build, in collaboration with the European Community Research and Training Network on *Adaptive Optics for Extremely Large Telescopes, a MCAO demonstrator*<sup>8</sup> (called MAD) before the end of the OWL feasibility study. The MAD instrument will have both a multi Shack-Hartmann WFS and LO WFS. It will be installed at a visitor Nasmyth focus of the VLT.

After an extensive description of the LO WFS concept, we present in the following the LO WFS part of the MAD instrument. We describe in particular the optical and mechanical design, the simulated performance of such a system and provide a time schedule for the instrument.

## 2. THE LAYER ORIENTED FOR MAD: TECHNICAL ISSUES

Since the MAD instrument will be installed on the Nasmyth focus of a VLT, the focal plane is assumed to be telecentric flat with a F/20 ratio. The LO WFS for MAD is a MCAO WFS composed of two detectors conjugated respectively to the ground and to 8.5km altitudes. The two DMs will be used for both the LO WFS and the Multi Shack-Hartmann WFS. The goal is to compensate for the phase distortion over a 2' FoV; the instrument will have eight pyramids to sense the light of eight guide stars. In the initial design of MAD<sup>12</sup>, there were two problems:

- i) the large size of pupil images coupled with the very small size of the detector chosen ESO
- ii) the absence in the MAD optical design of an intermediate pupil plane needed to introduce the tip-tilt system which modulates the image on the pyramid pin.

This is why two new concepts have been introduced in the LO WFS for MAD<sup>19</sup>: in order to reduce the re-imaged pupil we proposed the star enlarger<sup>20</sup> system and to solve the modulation problem we initially considered a diffusing plate<sup>21</sup>. Before building the LO WFS for MAD we tested and verified the LO concept of star pupils superimposition and the sensing of the phase distortion in open loop on a prototype. We refer to Farinato et al.<sup>22</sup> for a description of these tests and we focus on the optical and mechanical design of the LO WFS itself.

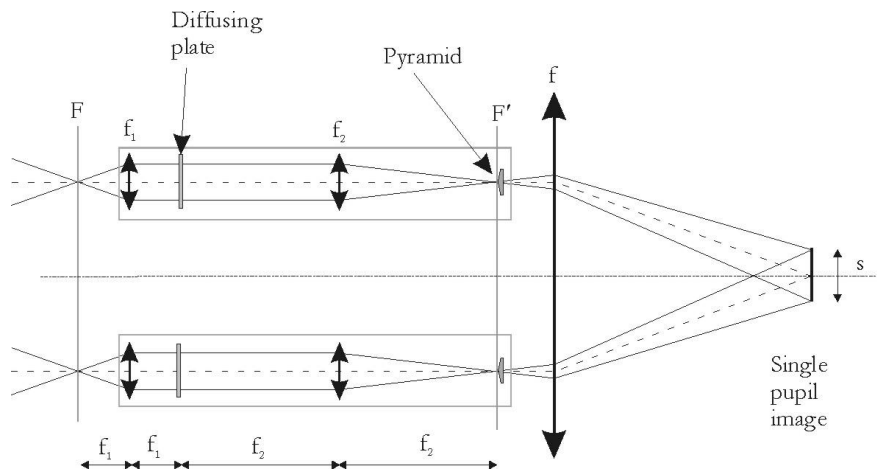
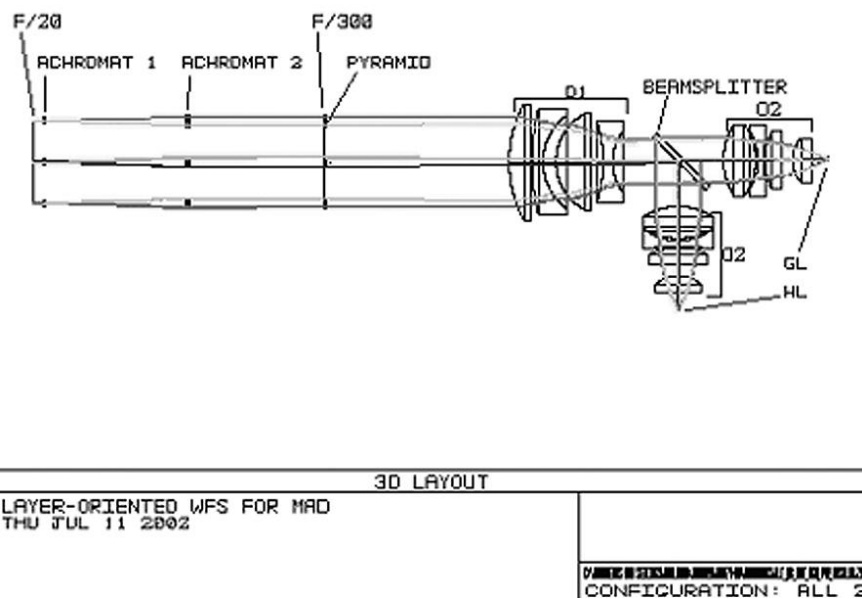


Figure 1. The LO WFS design concept.

## THE OPTICAL DESIGN

The star enlarger concept is used in the LO WFS design. Two lenses are introduced on each reference guide star path to enlarge<sup>20</sup> their focal ratio *individually* rather than collectively. As a result, the pupil size, which is inversely proportional to the focal ratio, can be arbitrarily shrunk, while the distance between the various stars across the covered FoV remains unchanged. The layout is shown in Figure 1.

The focal plane before the LOWFS is indicated by the vertical gray line. The incoming beam reaches the system in telecentric mode at a focal ratio  $F$ . The beam of each reference star is collimated by a lens of focal length  $f_1$  producing a small pupil image for each sensed star. A second lens of focal length  $f_2$ , placed a distance  $f_2$  to the right of the intermediate pupil (the exit pupil remains at infinity), forms an enlarged image of the reference star with an equivalent focal ratio  $F' = kF$ , where the enlarging factor is given by  $k = f_2/f_1$ .



**Figure 2. Optical layout of the LOWFS. Three star enlargers are shown. O1 and O2 are the two groups of lenses forming the pupil re-imager. GL and HL represent the ground and the high-altitude layer detectors.**

A pyramid can be placed at this position in order to split the light in four beams which are focused by an objective of focal length  $f$  onto four pupil images. The re-imaged pupils corresponding to different reference stars are collected by the objective, which optically co-adds the light of the stars. The size of each re-imaged pupil is  $s = f/F'$ . We will use two 1.536mm EEV50 CCDs, on which each single re-imaged pupil will have a diameter of 0.388mm. This dimension has been obtained after a careful optimization of the three lenses focal lengths and of the pyramid angle. These four parameters are given in Table 1 and the overall design is shown in Figure 2.

Parameter	Value
$f_1$	10 mm
$f_2$	150 mm
$f$	115.7 mm
$\beta$	0.605°

**Table 1. Main parameters of the LOWFS optical design;  $\beta$  represents the angular deviation of the beams produced by the pyramid.**

We originally planned to use a diffusing plate<sup>20</sup> instead of modulating the pyramid pin. This plate would have been inserted in the star enlargers in the image plane between the two achromat lenses as shown in Figure 1 but after recent simulations<sup>22</sup> and measurements on the sky<sup>23</sup> obtained at the TNG, we decided not to use any modulating system.

The pyramid prism is made in BK7 glass and has a vertex angle of  $\alpha = 1.176$ . The two star enlarger achromats are commercial ones. The 8-lenses pupil re-imager has been optimized in the full wavelength range 0.45 - 0.95 $\mu$ m with uniform weighting. The objective is composed of two groups of lenses: the beam compressor which reduces the beam cross section while collimating it; the second group focuses the beam at  $F/1.05$  ratio. A convenient space of 125mm is left between the two lens groups in order to insert the beam splitter for the ground and high altitude channels. Due to the broad wavelength range of the system, the optical performance is mainly limited by chromatic effects. The Modulation Transfer Function (MTF) of the objective gives an indication on the system sensitivity to aberrations of a given spatial frequency. The MTF of the objective is always above 90% for all the frequencies up to  $f_c \approx 21$  lines/mm (the inverse of the pupil sub-aperture size).

### THE LO WFS DESIGN

The overall instrument is approximately a 600 $\times$ 600 $\times$ 1000mm box which will be installed above the MAD bench. This box is divided into two parts: the lower mechanical structure contains the star enlargers and their motion system and the higher mechanical structure supports the re-imaging objectives and the refocusing unit.

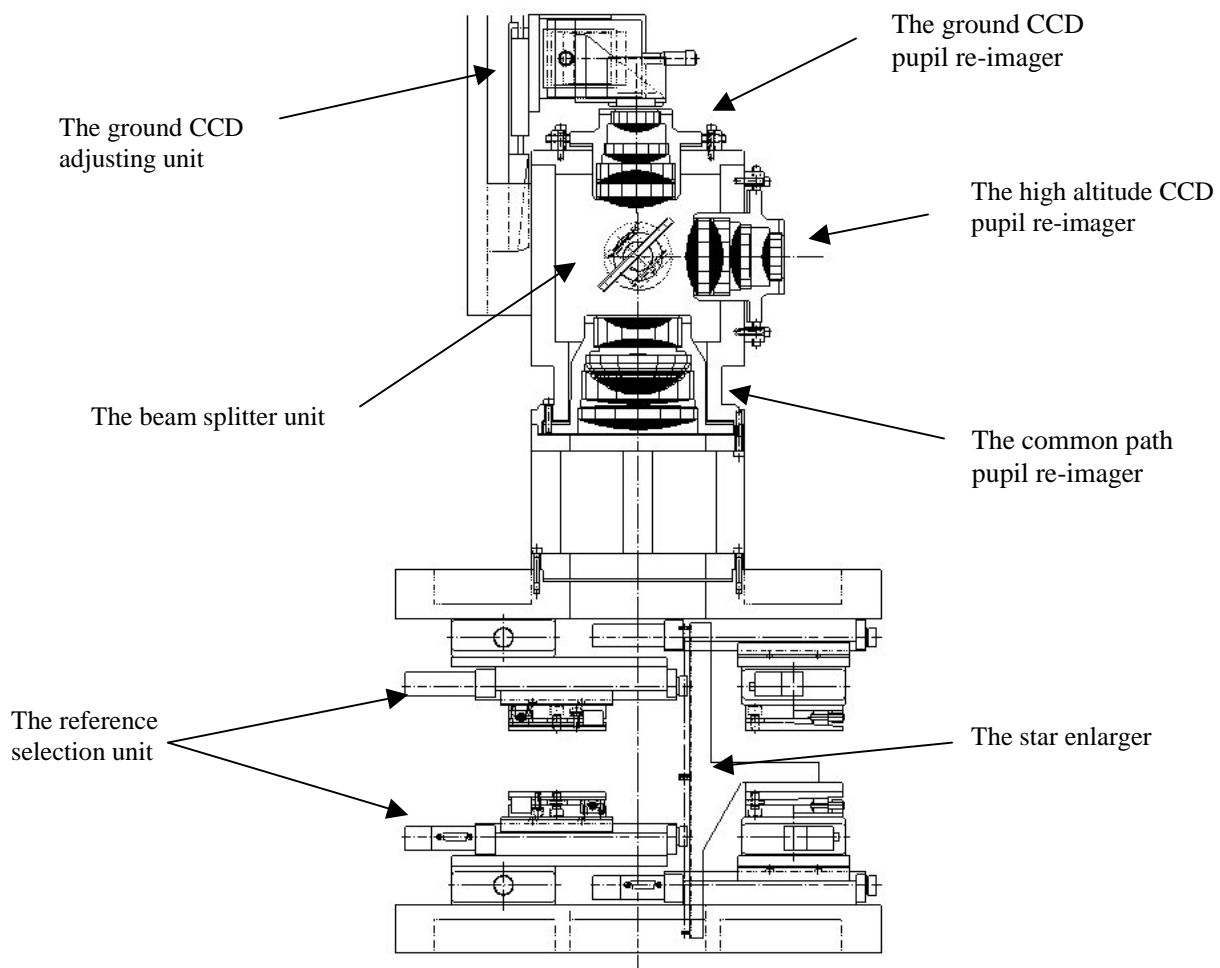
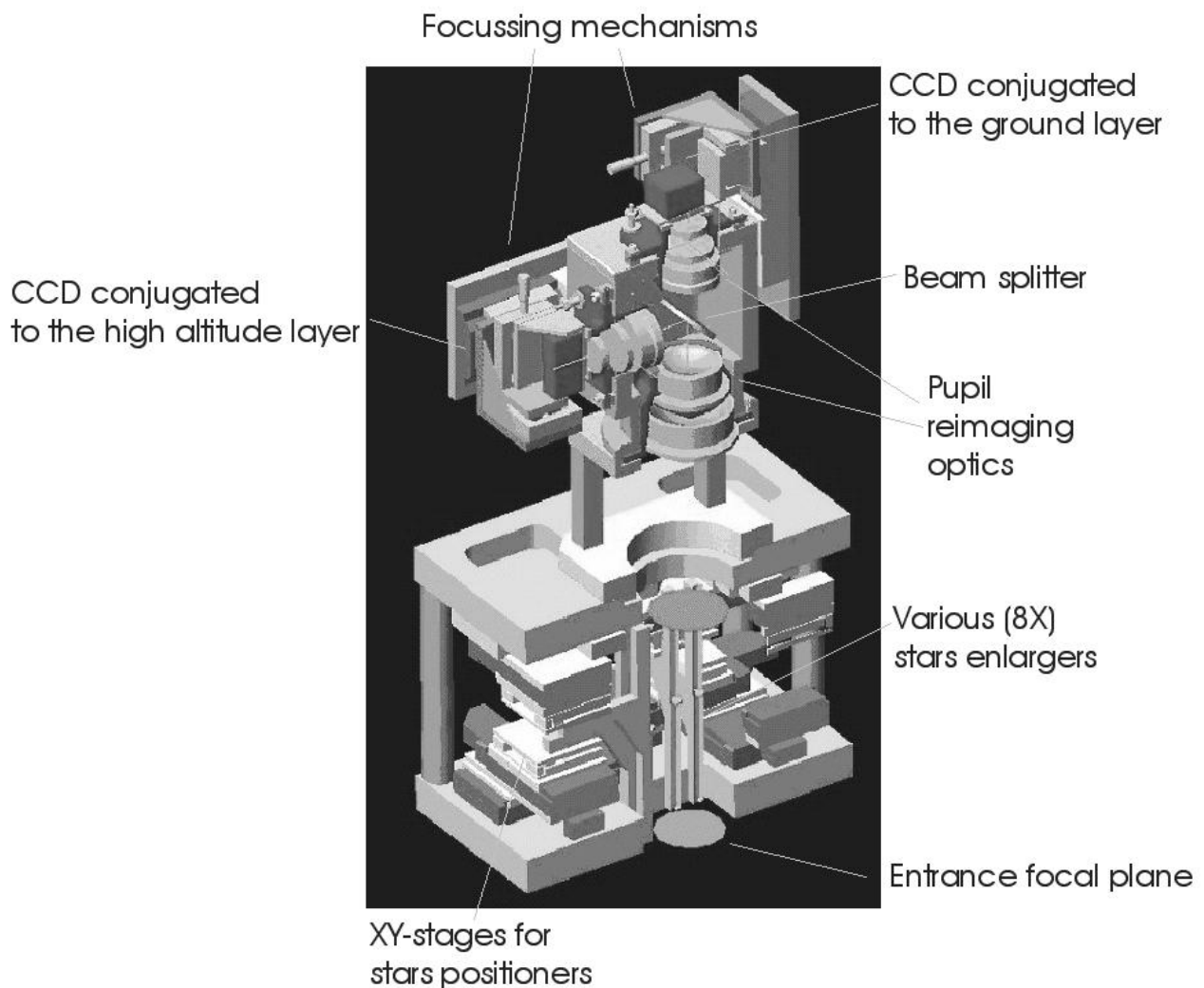


Figure 3. A side view of the Layer-Oriented WFS Box

The two CCD heads are mounted one at the top and the other on a side of the higher mechanical structure. For practical reasons, the optical path is vertical. The reference guide stars light coming from the bottom of the box is caught by the star enlargers. The star enlargers positioning is performed using two motorized linear stages for each of them. A maximum of eight reference stars can be selected by the eight star enlargers. Since the linear stages have to position the star enlargers with a high precision, we decided to place all of them horizontally. In Figure 3 one can see 8 of the 16 linear stages: 4 on the base plate of the main structure and 4 mounted up side-down on the top plate of the lower mechanical structure. The pyramids placed at the top of the star enlargers split the image into four parts. These 8 groups of 4 pupil images are first collimated by the common-path pupil re-imager, then the light is divided by the beam splitter between the ground and the high pupil re-imagers. These second groups of lenses re-image the pupil on a plane conjugated to the ground layer and to the high altitude layer. A 3D view of the instrument is shown in Figure 4.



**Figure 4. : 3D view of the LOWFS.**

From the electronic point of view the system is very easy: there are 18 motorized linear stages to be controlled (16 for the star enlargers positioning and 2 for the CDDs focus adjustments) the electronic control of which will be provided by ESO (standard MCAON boards) .

The software has to allocate one star enlarger to each reference guide stars so that there are at most two stars per quadrant. This is equivalent to find a coordinate transformation: in the most general case consisting of a shift in X,Y plane plus a rotation around Z. Shift in X,Y then translates into telescope offsets while rotations can be mapped to derotator offsets. To avoid any star enlarger collision, a metal ring is placed around every star enlarger: if one ring touches a metallic part, the corresponding X-Y stages are stopped.

### 3. SIMULATION OF THE LO WFS: PERFORMANCE ANALYSIS

We developed a simulation code able to reproduce the main characteristics of an MCAO LO module like MAD. This code written in IDL (Interactive Data Language) was first described in Ragazzoni, Farinato & Marchetti<sup>11</sup> in 2000 and after in Tordi, Ragazzoni & Diolaiti<sup>25</sup>. A script file defining the overall system properties (telescope characterization, AO system definition, wavefront sensing and correction parameters) is read by the code during its initialization phase. The simulation code allows to reproduce the behavior of either a classic AO or an MCAO system in a LO way.

The atmosphere is simulated by 7 phase screen layers generated using the usual Kolmogorov spectrum<sup>26</sup> and adding some sub-harmonics for a better match of the spectrum. The atmosphere evolution is simulated by shifting phase screens for each time step  $\Delta t$ . The integration time is an entire number of time steps. After one integration the code computes the reconstructed layers and deduces the DMs shapes (using the DM modes basis) which are subtracted from the wavefronts at the next step.

The 59 modes shapes of the DM provided by ESO have been introduced in the simulation in order to produce a realistic DM response. The 7 layers Paranal atmosphere model (see Table 2) is simulated using a seeing value in the V band of 0.73'' equivalent to an overall  $r_{0,V}$  of 0.141m observing at 30 degrees from the Zenith (in the K band at  $2.2\mu\text{m}$   $r_{0,K}$  is scaled to 0.834 m). Table 3 and Table 4 contain the main parameters of the simulation. The beam splitter used in the simulation divides the light into half for the high layer CCD and half for the ground CCD.

Layer	Altitude [m]	D/ $r_0$ @ K	Wind [ $\text{m/s}$ ]
1	0	7.38	6.6
2	1800	2.11	12.4
3	3200	2.67	8.0
4	5800	1.28	33.7
5	7400	1.05	23.2
6	13000	2.11	22.2
7	15800	0.77	8.0

**Table 2. Atmospheric parameters. The values refer to the Zenith while we simulate a telescope pointing at 30° from the Zenith. The heights of the layers are multiplied by  $\cos(30^\circ)^{-1}$  and the  $r_0$  values have been updated.**

D (m)	FoV (arcmin)	$\lambda_{\text{science}}$ ( $\mu\text{m}$ )	$\lambda_{\text{WFS}}$ ( $\mu\text{m}$ )	$\Delta\lambda_{\text{WFS}}$ ( $\mu\text{m}$ )	$M_{R, \text{sky}}$	Exposure Time (sec)	Overall QE	Delay time (sec)
8	2	2.2	0.55	0.4	20.0	> 1.0	0.1972	$3.0 \cdot 10^{-3}$

**Table 3. General parameters used in the simulation of the LO-WFS for MAD.**

DM	Altitude [m]	Gains	Sampling On WFS	Integration [ms]	RMS RON [ $\text{px}^{-1}\text{frame}^{-1}$ ]	Dark current [ $\text{px}^{-1}\text{s}^{-1}$ ]	DM Modes
1	0.0	0.6-0.9	8	2.5-20.0	$4.5 e^-$	$500 e^-$	59
2	8500.	0.6-0.9	7	2.5-40.0	$3.5 e^-$	$500 e^-$	43

**Table 4. AO system parameters. The binning used is 2x2 for the ground layer DM and 4x4 for the high layer DM.**

Since the LO WFS optically co-adds the reference star light on the WFS plane, we must use the integrated magnitude instead of individual guide stars magnitude to estimate the performance of the LO WFS with different number of guide stars (the integrated V magnitude is the equivalent star magnitude that would provide the same photon number than the one received from all the guide stars). The LO WFS performance has been studied with 3, 6 and 8 guide stars chosen in a 2' FoV. For the 3 guide stars case, we placed the star in a quasi symmetric position while for the 6 and 8 guide stars cases, we selected two real asterisms and scaled the guide star magnitudes in order to have a 12<sup>th</sup> integrated magnitude. Figure 5, Figure 6 and Figure 7 show the Strehl ratio map obtained after 1s of integration.

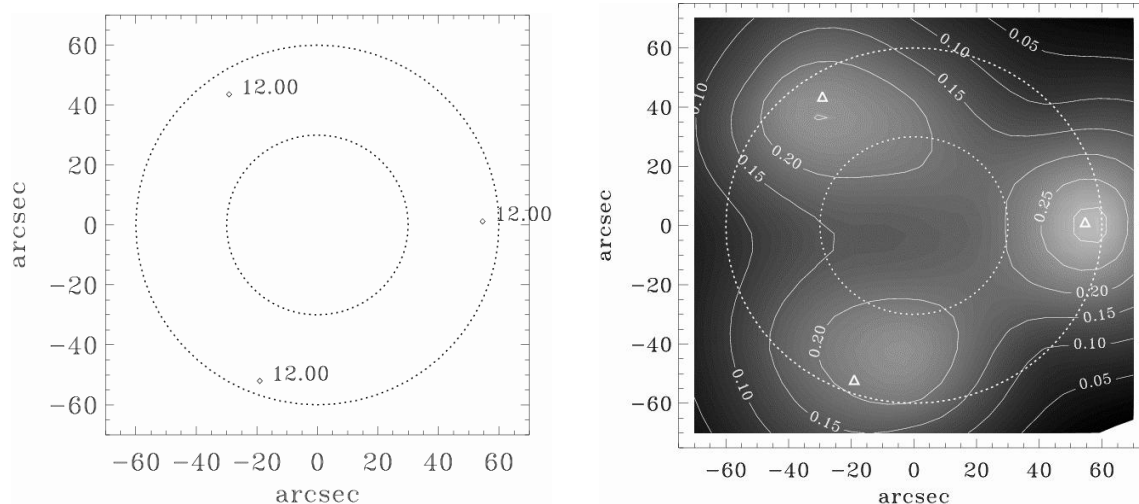


**Figure 5. Left panel: guide stars configuration and magnitudes. The two dashed circles show 1' and 2' FoV. Right panel: long exposure Strehl ratio map. The guide star positions are indicated by a triangle while the 1' and 2' FoV are shown by two dashed circles.**

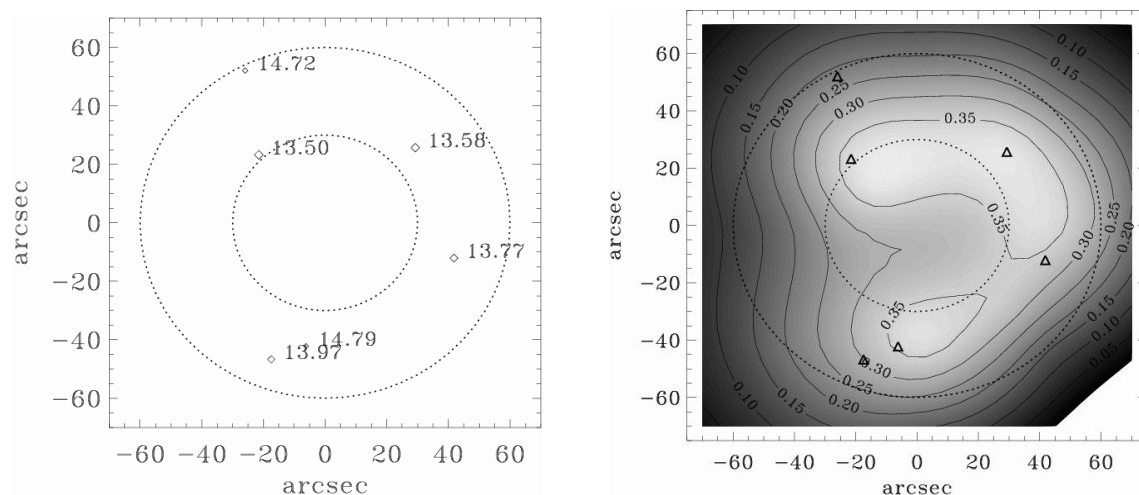


**Figure 6. Left panel: guide stars configuration and magnitudes. The two dashed circles show 1' and 2' FoV. Right panel: long exposure Strehl ratio map. The guide star positions are indicated by a triangle while the 1' and 2' FoV are shown by two dashed circles.**

The cases with 6 or 8 stars show a better performance of the system compared with the 3 stars case: the long exposure Strehl actually increases of 25% (from 0.3 to 0.4) even with very faint reference stars (magnitudes range going from 13.5 to 16.1 in the case of 8 guide stars).

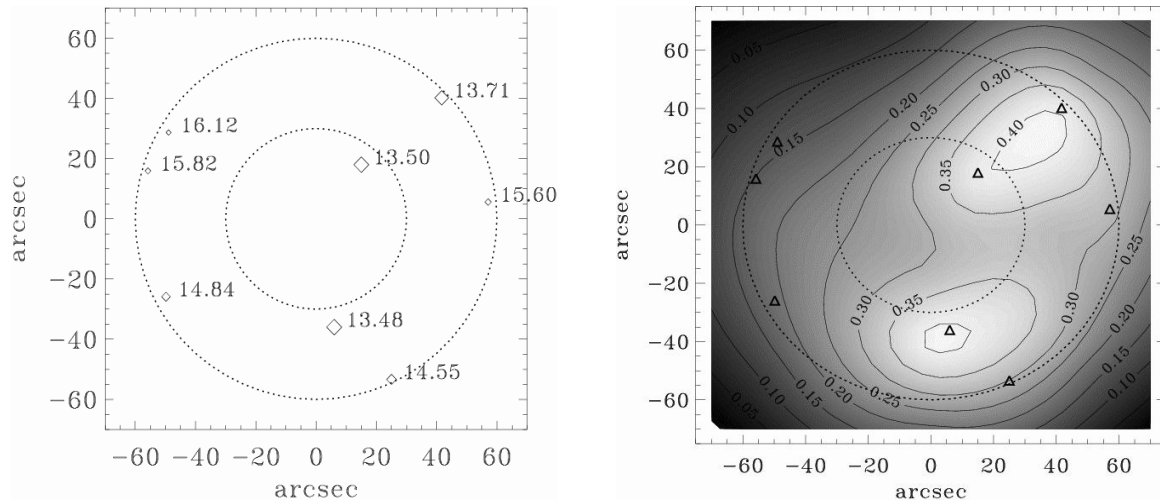


**Figure 7. On the left side: guide stars configuration and magnitudes. The two dashed circles show 1' and 2' FoV. On the right side, long exposure Strehl ratio map. The guide star position are indicated by a triangle while the 1' and 2' FoV are shown by two dashed circles.**

Number GS	$\Delta t$ integration on WF sensors	$\Delta t$ long exposure	Gains	SR on axis long exp.	Max SR long exp.	Max Instant. SR	$\sigma_{SR}$ over FoV	$\Delta$ SR over FoV
3	2.5 ms, 20 ms	2 sec	0.6, 0.6	0.16	0.31	0.51	0.06	0.26
6	5 ms, 10 ms	1.5 sec	0.6, 0.6	0.31	0.40	0.53	0.05	0.33
8	5 ms, 10 ms	1.5 sec	0.6, 0.6	0.30	0.41	0.57	0.06	0.35

**Table 5. Results obtained with a 12<sup>th</sup> integrated magnitude. The results correspond to the Strehl ratio map given in Figure 5, Figure 6 and Figure 7.**

We estimated the Strehl ratio with the 8 guide stars asterism for different integrated magnitudes and found that for a 14<sup>th</sup> integrated magnitude, we reach 0.28 long exposure Strehl ratio with guide stars individual magnitude being between 15.5 and 18.1.

#### 4. PROJECT STATUS

The first phase of the project was to demonstrate the LO concept in the laboratory in open loop. We built a prototype version of the LO WFS for MAD and tested both technical issues like star enlargers positioning and pupils superimposition of the different reference stars, and conceptual issues like wavefront sensing and phase reconstruction. All the tests are described in Farinato et al.<sup>22</sup>.

We are now entering in the manufacturing phase of the LO WFS. We are about to order the mechanical structure to the Tommelleri SPA (Verona, Italy) and the objective to SILO (Firenze, Italy). Integration and test phase should begin in Florence in November. Then the system will be mounted on the MAD bench and tested at ESO Garching at the beginning of next year (around March 2003). The acceptance test in Garching should be held in November 2003 before going to the VLT in December 2003. The test phase at Paranal will begin in January 2004 and the commissioning phase for the entire MAD instrument is foreseen to be finished by June 2004.

## ACKNOWLEDGMENTS

This work has been partially funded by the European Research and Training Network *Adaptive Optics for Extremely Large Telescopes* with Contract HPRN-CT-2000-00147.

## REFERENCES

1. J. M. Beckers, "The NOAO/ADP adaptive optics program and its application to solar physics", *Workshop on Adaptive Optics in Solar Observations*, F. Merkle, O. Engvold, R. Falomo Editions, LEST Technical Report 28, 55, 1987.
2. J. M. Beckers, "Increasing the size of the isoplanatic patch with Multi-conjugate adaptive optics", *Proceedings on Very Large Telescopes and their instrumentation*, M.-H. Ulrich Edition, 30, 693, ESO Proceedings, Garching, 1988.
3. B. L. Ellerbroek, "First-order performance evaluation of adaptive-optics systems for atmospheric-turbulence compensation in extended-field-of-view astronomical telescopes", *J. Opt. Soc. Am. A*, **11**, 783, 1994.
4. D. C. Johnston and B. M. Welsh, "Analysis of multiconjugate adaptive optics", *J. Opt. Soc. Am. A*, **11**, 394, 1994.
5. M. Le Louarn and M. Tallon, "Analysis of modes and behavior of a multiconjugate adaptive optics system", *J. Opt. Soc. Am. A*, **19**, 912, 2002
6. E. Diolaiti, R. Ragazzoni and M. Tordi, "Closed loop performance of a layer-oriented multi-conjugate adaptive optics system", *A&A*, **372**, 710, 2001.
7. B. J. Bauman, D. T. Gavel, L. M. Flath, R. L. Hurd, C. E. Max, S. S. Olivier, "Proposed multiconjugate adaptive optics experiment at Lick Observatory", *Adaptive Optics Systems and Technology II*, Robert K. Tyson; Domenico Bonaccini; Michael C. Roggemann; Eds., Proc. SPIE Vol. 4494, p. 81, 2002.
8. B. L. Ellerbroek, F. J. Rigaut, C. Boyer, C. D'Orgeville, M. R. Hunten, Multiconjugate adaptive optics for Gemini-South, *Adaptive Optics System Technologies*, SPIE Proceedings, 4839, article number [4839-07], 2002.
9. E. Marchetti, N. N. Hubin, E. Fedrigo, R. Donaldson, R. Conan, M. Le Louarn, B. Delabre, F. Franza, D. Baade, C. Cavadore, A. Balestra, J.-L. Lizon, R. Ragazzoni, J. Farinato, E. Vernet-Viard, E. Diolaiti, D. J. Butler, S. Hippler, A. Amorin, "MAD the ESO multiconjugate Adaptive Optics demonstrator", *Adaptive Optics System Technologies*, SPIE Proceedings, 4839, article number [4839-38], 2002.
10. R. Ragazzoni, T. Herbst, D. Andersen, P. Bizenberger, H. W. Rix, R.R. Rohloff, C. Arcidiacono, E. Diolaiti, S. Esposito, J. Farinato, A. Riccardi, E. Vernet Viard, P. Salinari, "NIRVANA: a visible MCAO for LBT", *Adaptive Optics System Technologies*, SPIE Proceedings, 4839, article number [4839-64], 2002.
11. R. Ragazzoni, "Adaptive optics for giant telescopes: NGS vs. LGS", *Proceedings of the Backaskog workshop on extremely large telescope*, T. Andersen, A. Ardeberg, R. Gilmozzi Editions, 57, 175, ESO Proc., Backaskog, 1999.
12. R. Ragazzoni, F. Farinato, E. Marchetti, "Adaptive optics for 100-m-class telescopes: new challenges require new solutions", *Adaptive Optical Systems Technology*, P. L. Wizinowich Editions, 4007, 1076, Proc. SPIE, Munich, 2000.
13. R. Ragazzoni, "Pupil plane wavefront sensing with an oscillating prism", *Journal of Modern Optics*, **43**, 289, 1996.
14. S. Esposito, O. Feeney, A. Riccardi, "Laboratory test of a pyramid wavefront sensor", *Adaptive Optical Systems Technology*, P. L. Wizinowich Editions, 4007, 416, Proc. SPIE, Munich, 2000.
15. R. Ragazzoni, A. Baruffolo, J. Farinato, A. Ghedina, E. Marchetti, S. Esposito, L. Fini, P. Ranfagni, F. Bortoletto, M. D'Alessandro, M. Ghigo, G. Crimi, "Final commissioning phase of the AdOpt@TNG module", *Adaptive Optical Systems Technology*, Peter L. Wizinowich Editions, 4007, 57, Proc. SPIE, Munich, 2000.
16. R. Ragazzoni, A. Ghedina, A. Baruffolo, E. Marchetti, J. Farinato, T. Niero, G. Crimi, M. Ghigo, "Testing the pyramid wavefront sensor on the sky", *Adaptive Optical Systems Technology*, Peter L. Wizinowich Editions, 4007, 423, Proc. SPIE, Munich, 2000.
17. S. Esposito and A. Riccardi, "Pyramid Wavefront Sensor behavior in partial correction Adaptive Optic systems", *A&A Letters*, **369**, L9, 2001.
18. R. Ragazzoni and J. Farinato, "Sensitivity of a pyramidal Wave Front sensor in closed loop Adaptive Optics", *A&A Letters*, **350**, L23, 1999.
19. R. Ragazzoni, E. Diolaiti, J. Farinato, E. Vernet, C. Arcidiacono, A. Baruffolo, "Layer-Oriented Wave Front Sensor Conceptual Design", ESO internal document, 2002.

20. R. Ragazzoni, E. Diolaiti, E. Vernet, J. Farinato, E. Marchetti, "Arbitrary small pupils in layer-oriented multi-conjugate adaptive optics", *to be submitted to PASP*, 2002.
21. R. Ragazzoni, E. Diolaiti, E. Vernet, "A pyramid wavefront sensor with no dynamic modulation", *Optics Communications*, **208**, pp 51-60, 2002.
22. J. Farinato, R. Ragazzoni, E. Diolaiti, E. Vernet Viard, A. Ghedina, M. Lecconi, M. Ghigo, G. Crimi, A. Baruffolo, R. Falomo, C. Arcidiacono, S. Esposito, M. Tordi, P. Rossettini, R. Tomelleri, "Layer-oriented adaptive optics: from drawings to metal", *Adaptive Optics System Technologies*, SPIE Proceedings, 4839, article number [4839-71], 2002.
23. J. Costa, R. Ragazzoni, S. Hippler, A. Ghedina, J. Farinato, "Is there need of any modulation in the pyramid wavefront sensor?", *Adaptive Optics System Technologies*, SPIE Proceedings, 4839, article number [4839-34], 2002.
24. A. Ghedina, M. Cecconi, R. Ragazzoni, J. Farinato, A. Baruffolo, G. Crimi, E. Diolaiti, S. Esposito, L. Fini, M. Ghigo, E. Marchetti, T. Niero, A. Puglisi, "Testing the pyramid wavefront sensor on the sky", *Adaptive Optics System Technologies*, SPIE Proceedings, 4839, article number [4839-105], 2002.
25. M. Tordi, R. Ragazzoni and E. Diolaiti, "Simulation of a Layer Oriented MCAO system", *Beyond Conventional Adaptive Optics Conference*, E. Vernet Viard, R. Ragazzoni, S. Esposito, N. Hubin Editions, 223, ESO Proceedings, Venice, 2001.
26. R. J. Noll, "Zernike polynomials and atmospheric turbulence", *JOSA*, **66**, 3, 207, 1976.